



1 **Nonlinear turnover rates of soil carbon following cultivation of native grasslands and**
2 **subsequent afforestation of croplands**

3

4 Guillermo Hernandez-Ramirez*

5 Department of Renewable Resources

6 University of Alberta

7 Edmonton, AB, T6G2R3

8 Canada

9 *Corresponding author. Tel.: +1 780 492 2428, E-mail address: ghernand@ualberta.ca.

10

11 Thomas J. Sauer

12 USDA-ARS,

13 National Laboratory for Agriculture and Environment,

14 Ames, IA 50011,

15 USA

16

17 Yury G. Chendev

18 Department of Natural Resources Management and Land Cadastre,

19 Belgorod State University,

20 85 Pobeda Street, Belgorod 308015,

21 Russia

22

23 Alexander N. Gennadiev

24 Lomonosov Moscow State University,

25 Faculty of Geography,

26 119991, Moscow, GSP-1, 1 Leninskiye Gory,

27 Russia



28 **Abstract**

29 Land use conversions can strongly impact soil organic matter (SOM) storage, which
30 creates paramount opportunities for sequestering atmospheric carbon into the soil. It is known
31 that land uses such as annual cropping and afforestation can decrease and increase SOM,
32 respectively; however, the rates of these changes over time remain elusive. This study focused on
33 extracting the kinetics (k) of turnover rates that describe these long-term changes in soil C
34 storage and also quantifying the sources of soil C. We used topsoil organic carbon density and
35 $\delta^{13}\text{C}$ isotopic composition data from multiple chronosequences and paired sites in Russia and
36 United States. Reconstruction of soil C storage trajectory over 250 years following conversion
37 from native grassland to continual annual cropland revealed a C depletion rate of 0.010 years^{-1}
38 (first-order k rate constant), which translates into a mean residence time (MRT) of 100 years
39 ($R^2 \geq 0.90$). Conversely, soil C accretion was observed over 70 years following afforestation of
40 annual croplands at a much faster k rate of 0.055 years^{-1} . The corresponding MRT was only 18
41 years ($R^2 = 0.997$) after a lag phase of 5 years. Over these 23 years of afforestation, trees
42 contributed 14 Mg C Ha^{-1} to soil C accrual in the 0 to 15 cm depth increment. This tree-C
43 contribution reached 22 Mg C Ha^{-1} at 70 years after tree planting. Over these 70 years of
44 afforestation, the proportion of tree-C to whole soil C increased to reach a sizeable 79%.
45 Furthermore, assuming steady state of soil C in the adjacent croplands, we also estimated that
46 45% of the prairie-C existent at time of tree planting was still present in the afforested soils 70
47 years later. As intrinsic of k modelling, the derived turnover rates that represent soil C changes
48 over time are nonlinear. Soil C changes were much more dynamic during the first decades
49 following a land use conversion than afterwards when the new land use system approached
50 equilibrium. Collectively, results substantiated that C sequestration in afforested lands is a



51 suitable means to proactively mitigate escalating climate change within a typical person's
52 lifetime, as indicated by MRTs of few decades.

53

54

55



56 **1 Introduction**

57 The global effects of escalating climate change are in part driven by land use choices.
58 Indeed, implementing certain land use changes can worsen or in other cases mitigate emissions
59 of greenhouse gases from terrestrial ecosystems to the atmosphere (Paustian et al., 1992; Post
60 and Kwon, 2000; Thilakarathna and Hernandez-Ramirez in press). Essentially, land use options
61 that unintentionally accelerate biological oxidation of soil organic matter (SOM) contribute over
62 time to atmospheric carbon dioxide concentrations (Sauer et al., 2007; Laganriere et al., 2010; Li
63 et al., 2018), providing a portion of the radiative forcing that has been causing part of the global
64 warming effect over the last decades (Guo and Gifford, 2002; Parry et al. 2007). Compared with
65 contrasting types of land use systems, annual croplands commonly showed SOM depletion and
66 marked reductions in soil C storage, in particular relative to their natural ecosystem counterparts
67 (Chendev et al., 2015b; Hebb et al., 2017; Kiani et al., 2017).

68 Contrary to the potentially detrimental effects of annual cropping on SOM accumulation
69 and overall soil quality (Guenette and Hernandez-Ramirez, 2018; Laganriere et al., 2010; Kiani et
70 al., in press), tree planting offer multiple environmental services and societal benefits
71 (Hernandez-Ramirez et al., 2012; Sauer et al., 2012; Zhang et al., 2020). For instance, removing
72 C from the atmosphere is a paramount contribution by trees (Guo and Gifford, 2002; Li et al.,
73 2012; Li et al., 2018). In effect, soil C accrual (Paul et al., 2002; Dhillon and Van Rees, 2017;
74 Khaleel et al., 2020) and stabilization (Hernandez-Ramirez et al., 2011; Wang et al., 2016;
75 Quesada et al., 2020) beneath trees have been recognized as an effective means for sequestering
76 atmospheric C. In addition to soil accruals, soil microbiology is sustained and diversified beneath
77 mature trees (Kiani et al., 2017). Additional functions by tree vegetation include improving air
78 quality, enhanced microclimate, and erosion control (Sauer et al., 2007; Hernandez-Ramirez et



79 al., 2012; Chendev et al., 2015b). Establishing agroforestry practices such as shelterbelt systems
80 within annual croplands can provide a balance between continual food production and tree
81 benefits with only a fraction of the landscape occupied by trees (Amadi et al., 2016; Dhillon and
82 Van Rees, 2017).

83 Sequestering C in soils is governed by the balance of inputs of plant C with biological-
84 mediated decomposition and stabilization processes (Hernandez-Ramirez et al., 2009; Kiani et
85 al., 2017; Li et al., 2018). This overall functioning of C-related biology and cycling in soils can
86 be described as the turnover of soil C. Collectively, SOM decomposition, mineralization, gains
87 and losses and net accrual can be numerically integrated into C turnover rates (Richter et al.,
88 1999; Hernandez-Ramirez et al., 2011; Xiong et al., 2020). For instance, dynamic rates of net
89 depletion of SOM pools caused by continual cropping or tree contributions to soil C accretion
90 and cycling under afforestation can both be captured as C turnover rates (Guo and Gifford, 2002;
91 Hu et al. 2013). However, the outcomes of how slow or fast the accrual of SOM takes place as a
92 function of land use conversions need to be assessed in the long term, as this will inform how
93 lasting these effects are (Paustian et al., 1992; Hernandez-Ramirez et al., 2011). Indeed,
94 understanding long-term changes in SOM storage, instead of the results from a single point in
95 time, is highly valued knowledge (Paustian et al., 1992; Richter et al., 1999; Guo and Gifford,
96 2002). Extracting and making available in the literature the long-term turnover rates of SOM
97 depletion or accretion can enable useful projections of future soil C sequestration as a function of
98 implementing land use changes. Our study endeavors to address and fill this knowledge gap.

99 In this study, we compiled soil C storage data from several field sites comparing land use
100 systems in Russia and United States (Chendev et al., 2015a, 2015b) in conjunction with
101 published (Hernandez-Ramirez et al., 2011) and newly-available soil ^{13}C isotope data. Based on



102 these data assemblage, we now focused on evaluating the long-term turnover rates of soil C as a
103 function of land use changes from native grasslands to annual croplands and subsequent
104 converting annual croplands into afforestation. We aimed at extracting turnover rates of soil C
105 depletion or accretion, which can enable future predictions of soil C storage depending on land
106 use systems. Also, our study quantified and documented the contributions of tree biomass-C to
107 soil C that was newly-acrued following afforestation. We further examined the stage and net
108 losses of the C that existent in the soil under annual croplands prior to tree planting.

109

110 **2 Materials and Methods**

111 **2.1 Chronosequences from native grasslands to annual croplands in Russia**

112 Three long-term chronosequences of land use conversion (i.e., a range of different
113 duration of cultivation) were used for extracting turnover parameters. These land use
114 chronosequences were situated in Belgorod oblast, Russia within the districts of Prokhorovskiy
115 (50°57' N, 36°44' E), Gubkinskiy (51°03' N, 37°22' E) and Ivnyanskiy (51°06' N, 36°24' E) as
116 previously described by Chendev et al. (2015a) (Fig. 1). Following chronosequence methods as
117 described by Laganier et al. (2010), each chronosequence had four or five age-sites
118 encompassing a native grassland site that represented the time zero of conversion from grassland
119 to annual cropland. These native grasslands were undisturbed steppe dominated by plant species
120 with C3 photosynthetic pathway. The ages of the cropland sites were established through
121 historical records and geographic approaches described by Chendev et al. (2012, 2015b).
122 Composite soil samples (3 subsamples per sample) with at least 12 sampling locations per age-
123 site were collected using the core method in 10 cm depth increments. Additional information
124 about these sites is available at Chendev et al. (2015a), while the focus in our study remains on



125 developing models and extracting parameters of C turnover rates. Typical annual crops species
126 included cereals, sunflower (*Helianthus annuus*) and beet (*Beta vulgaris*) managed under
127 conventional tillage operations. Within the study region, soils were classified as loamy
128 Chernozems (Russian Soil Classification System), annual precipitation ranged between 480 and
129 580 mm and air temperature between 5.3 and 5.8 °C (Chendev et al., 2015a).

130 Soil organic C mass density for the 0 to 30 cm depth was calculated as the sum of
131 products of organic C concentration (Hernandez-Ramirez et al., 2009), bulk density and soil
132 layer thickness, with units of Mg C ha⁻¹.

133 First-order kinetic modelling follows:

$$134 \quad C_{(t)} = C_e + (C_o - C_e) e^{-kt} \quad [1]$$

135 where C_e is soil C storage at the oldest cropland site within each chronosequence which was
136 assumed to be at new dynamic equilibrium (i.e., C inputs = C outputs), C_o is soil C storage at the
137 native grassland site which was assumed to be the initial time of land use conversion from native
138 grassland to annual croplands (time zero), k is the fitted first-order kinetic rate constant (yr⁻¹),
139 which is equivalent to C turnover rate or net C mineralization (in the case of net C decreases),
140 and t stands for time (yr). In the case of increases in soil C over time, turnover rates become
141 equivalent to accretion rates. It is possible to model the soil C storage for each year, and hence,
142 the difference between consecutive years provides an estimation of the annual net C change (Mg
143 C ha⁻¹ yr⁻¹). In addition to balance between C inputs and C outputs, first-order kinetic modelling
144 also assumed steady state conditions (i.e., $\delta C/\delta t = 0$). At the selected sampling sites, given the
145 flat topography, we also assumed negligible C removals or additions due to erosion or
146 deposition.



147 Mean residence time (MRT) of organic C in the soil was calculated as reciprocal of k.

148 Concomitantly, half-life of organic C in the soil was calculated as follows:

149 $\text{Half-life} = \ln(2)/k$ [2]

150 Note that under equilibrium, C output_e is also equivalent to C input_e, and they correspond to the
151 annual C that enters and exits the soil C pool, respectively.

152 The performance of the derived first-order kinetic modelling was evaluated with the
153 normalized root mean square error (RMSE_n) (Guenette and Hernandez-Ramirez, 2018; Kiani et
154 al., in press), coefficient of determination (R²) as well as a leave-one-out cross-validation of
155 predicted versus measured C. Within the cross-validation, we tested the regression coefficient
156 (β₁) of a linear regression established for predicted vs. measured C against the 1:1 line.

157 **2.2 Comparison of adjacent paired sites in Russia: native grasslands, annual croplands and** 158 **shelterbelts (trees)**

159 In addition to the three abovementioned chronosequences, three additional sites were
160 studies in Russia: Streletskaya Steppe situated within Kursk oblast (51°32' N, 36°05' E),
161 Yamskaya Steppe in Belgorod oblast (51°11' N, 37°37' E), and Kamennaya Steppe in Voronezh
162 oblast (51°02' N, 40°44' E) (Fig. 1). Soils at all these paired sites were classified as loamy
163 Chernozems. Following field methods as described by Laganriere et al. (2010), each site
164 encompassed adjacent locations representing three land uses: native grassland, annual croplands
165 and broadleaf shelterbelts, as described by Chendev et al. (2015b). Soil sample collections were
166 conducted similar as described above. Briefly, composite soil samples (3 subsamples per sample)
167 were collected from the native grassland (n= 6 composite soil samples), annual croplands (24)
168 and shelterbelts (18) in summer 2012. At time of soil sample collection, the ages of the annual
169 croplands in Streletskaya and Yamskaya were at least 140 years, and at least 145 years of age in



170 Kamennaya. In all three sites, the shelterbelts had been planted 55 years prior to soil sample
171 collection. Tree species in the shelterbelts include silver birch (*Betula verrucosa*) and black
172 poplar (*Populus nigra*) at the Streletskaya site, American maple (*Acer negundo*) at the Yamskaya
173 site, and balsam poplar (*Populus balsamifera*) and English oak (*Quercus robur*) at the
174 Kamennaya site. Normal mean annual precipitations at Streletskaya, Yamskaya and Kamennaya
175 correspond to 580, 530 and 480 mm yr⁻¹, respectively.

176 It is noted that although trees at the Streletskaya, Yamskaya and Kamennaya sites were
177 planted 55 years prior to soil sample collection, for first-order kinetics modelling purposes, the
178 tree-C contributions to soil C accrual were accounted beginning from 50 years prior to soil
179 sample collection. This assumption is based on a literature review by Paul et al. (2002) who
180 suggested a lag phase of 5 years for tree-C contributions to effective start contributing to net
181 storage of soil C. Moreover, because of the uncertainty of how close the afforested soils were to
182 steady state and equilibrium of soil C storage, we evaluated two scenarios of first-order kinetics
183 modelling using Eq. [1]. We assessed trajectory ‘A’ under the premise that full steady state has
184 been reached at time of soil sample collection, and also trajectory ‘B’ where we assumed that the
185 C storage in these afforested soils had asymptotically reached 95% of the theoretical equilibrium
186 or ceiling capacity. We reported both trajectories and their associated C accretion rates (k).

187 **2.3 Pairwise comparisons in United States: annual croplands and afforestation**

188 Three field sites were studied within the Northern Great Plains of United States near the
189 cities of Huron (South Dakota, 44°15′ N, 98° 15′ W), Norfolk (Nebraska, 42° 03′ N, 97° 22′ W)
190 and Mead (Nebraska, 41°9′ N, 96°29′ W) (Fig. 1). While the focus remained on investigating the
191 turnover rates of soil C as a function of land use changes, it is noted that pedogenic ages of the
192 soils sampled in United States were relatively shorter than the soils studied in Russian sites. This



193 is because of the differences in geological times of parent materials exposure on the ground
194 surface between geographic regions since the sites in United States experienced the last
195 glaciation (i.e., Wisconsin glaciation).

196 The three sites in United States encompassed afforested areas and adjacent annual
197 croplands, co-located in paired sites as Laganriere et al. (2010). The native vegetation at the sites
198 had been tall prairie (e.g., big bluestem *Andropogon gerardii* Vitman), which had been converted
199 into annual croplands, and trees were subsequently planted in areas of the croplands.

200 Afforestation took the forms of shelterbelts in Norfolk and Mead, and a forest plantation in
201 Huron. The Huron site also had an adjacent field with a representative undisturbed native prairie,
202 which was also sampled as a reference. In contrast to the long-term croplands in Norfolk and
203 Mead, the cropland at Huron had only 21 years since conversion from native grassland at time of
204 soil sample collection. Field sample collections were conducted in 2004 in Mead, and in 2012 in
205 both Norfolk and Huron. The trees had been planted 19, 35 and 70 years prior to soil sample
206 collections in Huron, Mead and Norfolk, respectively. Tree species included green ash (*Fraxinus*
207 *pennsylvanica* Marshall), red cedar (*Juniperus virginiana* L.), and oak (*Quercus macrocarpa*) in
208 Huron; red cedar, scotch pine (*Pinus sylvestris* L.), and cottonwood (*Populus deltoides* Bartram)
209 in Mead; Siberian elm (*Ulmus pumila*), red mulberry (*Morus rubra*), and cottonwood in Norfolk.
210 Annual croplands were managed under conventional farming practices. Annual crop species at
211 the study sites included wheat (*Triticum aestivum* L.), corn (*Zea mays* L.), soybean [*Glycine max*
212 (L.) Merr.], and sorghum (*Sorghum bicolor* L. Moench). An alfalfa (*Medicago sativa* L.) forage
213 field adjacent to the shelterbelt in Norfolk was also sampled. Normal annual precipitation in
214 Huron, Norfolk and Mead were 582, 696 and 747 mm yr⁻¹, respectively. Normal air temperature
215 in Huron, Norfolk and Mead were 7.7, 9.6, 9.9 °C, respectively. Soil textures were loamy sand in



216 Norfolk, sandy loam in Huron and silty clay loam in Mead, respectively. Soil pH were 6.1 in
217 Mead, 6.8 in Norfolk, and 7.0 in Huron.

218 Field methods of soil sample collections had previously been described in related reports
219 by Chendev et al. (2015a) for the Huron and Norfolk sites as well as by Sauer et al. (2007) for
220 Mead. Briefly, spatial grid patterns were established with composite samples (n= 4) collected
221 from each sampling location. Total grid sampling locations were 118 at Mead, 48 at Huron, and
222 42 at Norfolk. Plant tissue samples of the dominant species were also collected from each study
223 site.

224 Organic C concentration and $\delta^{13}\text{C}$ isotopic composition were determined in all soil and
225 plant samples via the dry combustion method using a Fison NA 15000 Elemental Analyzer
226 (ThermoQuest Corp., Austin, TX) interfaced to an isotope-ratio mass spectrometer Delta V
227 Advantage (Thermo Fisher Scientific, Waltham, MA). Pee Dee Belemnite was used as standard
228 and analytical precision of $\delta^{13}\text{C}$ measurements was 0.06‰. The $\delta^{13}\text{C}$ isotopic ratio was
229 expressed as:

$$230 \quad \delta^{13}\text{C} (\text{‰}) = \left[\left(\frac{^{13}\text{C}/^{12}\text{C} \text{ sample}}{^{13}\text{C}/^{12}\text{C} \text{ standard}} \right) - 1 \right] \times 1000 \quad [3]$$

231 When integrating multiple soil layers of a profile, averages of $\delta^{13}\text{C}$ were weighted by the
232 soil C mass density at the corresponding soil layers.

233 Prior to land use conversion to croplands, the native grasslands in United States were
234 undisturbed and dominated by plant species with C4 photosynthetic pathway, with certain mixed
235 presence of C3 species. Based on this legacy contribution of prairie vegetation to soil C over the
236 Holocene, and assuming that net contributions to soil C storage were negligible during annual
237 cropping stages, approaches based on stable isotope signatures became feasible in these three
238 sites in United States. This method enabled us to examine the sources of soil C and also derive



239 the turnover rates of these soil C sources. This primarily applies because trees are C3 species.
240 This approach assumed that the differences in ^{13}C isotopic signatures between C4-C3 mixed
241 (native grassland) and C3 (trees) overrides any potential differential effect of C isotopic
242 fractionations during SOM decomposition of C3 vs. C4 substrates, between aboveground and
243 below ground plant materials (roots vs. litter), or because of SOM interactions with soil mineral
244 surfaces (Martin et al., 1990; Hernandez-Ramirez et al., 2011). Assuming mass conservation, the
245 measured soil C storages were allocated into two sources: new tree-C and remaining prairie-C
246 (native soil) as follows:

$$247 \text{ Tree-C} + \text{Prairie-C} = 1 \quad [4]$$

$$248 \text{ Tree-C} = (\delta^{13}\text{C}_{\text{afforested soil}} - \delta^{13}\text{C}_{\text{native soil}}) / (\delta^{13}\text{C}_{\text{tree}} - \delta^{13}\text{C}_{\text{native soil}}) \quad [5]$$

249 It was inferred that all soil C different from the C identified as new ‘Tree-C’ was
250 preexisting soil C attributable to remaining ‘Prairie-C’. Likewise, we assumed that the ‘ $\delta^{13}\text{C}$
251 native soil’ were represented reasonably well by the $\delta^{13}\text{C}$ measured in soil samples taken from
252 the annually-cropped fields adjacent to the afforested soils. Although they were adjacent, the
253 sampling locations providing the ‘ $\delta^{13}\text{C}$ native soil’ were sufficiently distant from afforested areas
254 to preclude influence of trees on soil $\delta^{13}\text{C}$. The ‘ $\delta^{13}\text{C}$ native soil’ were -17.3‰ in Huron, -17.0‰
255 in Mead, and -17.5‰ in Norfolk, which are noted to be consistent with each other as these sites
256 share a common natural history of tall prairie native vegetation. These ‘ $\delta^{13}\text{C}$ native soil’ are also
257 consistent with earlier measurements in prairie soils by Follett et al. (1997) and Hernandez-
258 Ramirez et al. (2011). Furthermore, the $\delta^{13}\text{C}$ measured in tree samples averaged -27.6‰ in
259 Huron, -26.6‰ in Mead, and -27.9‰ in Norfolk as typical isotopic compositions of C3 plant
260 species. At the Norfolk site, tissue samples of alfalfa canopy yielded -27.4‰. Also, in Norfolk,
261 ‘ $\delta^{13}\text{C}$ afforested soil’ included all data from the soil samples taken within 10 m north and 10 m



262 south from the center of the shelterbelt. In Huron, ‘ $\delta^{13}\text{C}$ afforested soil’ sample included all data
263 from soil samples taken at least 17 m away from the edge between the forest plantation and the
264 adjacent annually-cropped field. In Mead, as earlier presented by Hernandez-Ramirez et al.
265 (2011), ‘ $\delta^{13}\text{C}$ afforested soil’ sample included all data from soil samples collected between the
266 existing two tree rows.

267 The mass densities of soil C derived from new tree-C and remaining prairie-C were
268 calculated by multiplying whole soil C storage beneath the trees with the corresponding fractions
269 expressed in Eq. [4].

270 When assessing first-order kinetics modelling (Eq. [1]) of soil C beneath trees, we
271 assumed that the remaining prairie-C in afforested soils at time of soil sample collection was at
272 steady state and had also reached new equilibria in the case of the long-term annual croplands at
273 Norfolk and Mead. In the specific case of Huron, because the afforested soil had experienced
274 only two years of annual cropping prior to tree planting, we assumed that the native grassland
275 prior to land use conversion to annual cropping was at equilibrium and steady state.

276 Relationships between allocations of soil C sources (% tree-C, and % prairie-C) and time
277 since tree planting (years) were examined through linear regression analyses. Likewise, a similar
278 linear regression was developed for the proportions of remaining prairie-C in the afforested soils
279 relative to whole C present in the adjacent cropland soils. We used SigmaStat Version 4.0
280 software (Systat Software, San Jose, CA) and an α critical level of 0.05. Where error terms (\pm)
281 are presented, they correspond to the standard errors of the means.

282

283 **3 Results**

284 **3.1 Soil C after conversion of grasslands to cropland and then shelterbelt: Russian cases**



285 Long-term cultivation of native grasslands decreased soil organic C storage in a nonlinear
286 fashion (Fig. 2). Within each of the three available land use chronosequences (i.e., each
287 encompassing a range of different duration of cropping since land use conversion), the declining
288 trajectory of soil C was represented reasonably well by first-order kinetic modelling. (A). The
289 RMSEn were all lower than 4% and the R^2 were greater than 90%, which supports the suitable
290 performance of k models (Fig. 2A, Fig. 2B, and Fig. 2C). Likewise, cross-validation results of
291 cropland soils within the age range from 10 to 200 years further indicated the high accuracy of k
292 predictions when compared with the 1:1 agreement line. This was based on a non-significant t-
293 test with $\beta_1=1$ as null hypothesis (Fig. 2D).

294 Within the soil layer of 0 to 30 cm depth in the chronosequences in Belgorod, Russia,
295 turnover rates (k) of soil C ranged from 0.0091 to 0.0183 yr⁻¹ in Gubkinskiy and Prokhorovskiy,
296 respectively. Over the entire time spans of the three chronosequences, net soil C losses were in
297 the relatively narrow range from 31.2 Mg C ha⁻¹ in Prokhorovskiy (Fig. 2A) to 36.9 Mg C ha⁻¹ in
298 Gubkinskiy (Fig. 2B). Focusing on these losses of the preexisting soil C, the estimated lapses for
299 half of these C losses to take place was between 38 and 76 years after the time of land use
300 conversion from native grassland to annual cropland (Fig. 2A and Fig. 2B, respectively). It is
301 noted that new dynamic equilibria were assumed to have taken place in the oldest cropland soil
302 within each chronosequence (i.e., > 200 yrs) as part of first-order kinetics modelling.
303 Furthermore, when examining the assumption of steady state (i.e., $\delta C/\delta t = 0$), soil C trajectories
304 at both Prokhorovskiy and Ivnyanskiy sites showed reasonable approximations to this premise,
305 with relatively low annual C losses occurring towards the end of these chronosequences. On the
306 other hand, the Gubkinskiy site still exhibited vigorous C losses at the end of this
307 chronosequence, which can question steady state assumption at this site. In further details, the



308 trajectory at the Prokhorovskiy site showed estimated C losses of only 9.4 Kg C ha⁻¹ yr⁻¹ during
309 the last year of this chronosequence (Fig. 2A), which can be considered negligible and in clear
310 agreement with a steady state condition. Conversely, the last year of the Gubkinskiy
311 chronosequence still showed a C loss of 34.5 Kg C ha⁻¹ yr⁻¹. It is noteworthy that while these
312 annual C outputs typically take the form of soil respiratory losses (CO₂-C) that are resultant from
313 microbial mineralization of existing SOM. These estimations of net changes at near steady state
314 do not account for the CO₂ derived from the decomposition of recently-added plant residues, but
315 just the net change in SOM-C (Fig. 2A). For comparison purposes, the k-modelled trajectory of
316 the Prokhorovskiy chronosequence had estimated C losses of 566 Kg C ha⁻¹ yr⁻¹ during the very
317 first year after conversion from native grassland to annual cropland.

318 Afforestation implemented in the form of shelterbelts replenished soil C storage based on
319 assessed pairwise comparisons (Table 1). Cropping led to decreasing soil C relative to adjacent
320 native grasslands (Table 1), which was consistent with the results from chronosequences
321 described above (Fig. 2). Nevertheless, afforestation following cropping increased soil C accrual.
322 In further details, of the substantial soil C storage that had been depleted over time during annual
323 cropping (i.e., -18.9 ± 5.3 Mg C ha⁻¹), afforestation replenished on average 81% of these
324 cropping-induced C losses (Table 1). This replenishment of soil C by tree contributions was
325 observed across the three sites, but with certain variability. The Yamskaya site showed a
326 pronounced tree-induced replenishment of 138% of the lost soil C, which was even higher than
327 the native grassland in terms of soil C storage. On the other hand, at the Kamennaya site,
328 afforestation has only restored 5% of the soil C that had been lost during long-term cropping.

329 Using the insights gained from both chronosequences (Fig. 2) and pair site comparisons
330 (Table 1), we undertook the reconstruction of soil C storage progression in the 0 to 30 cm soil



331 layer since the land use conversion from native grassland to annual cropland and subsequently
332 into shelterbelt (Fig. 3). After normalizing all cropland-chronosequence data, turnover rates (k)
333 and first-order kinetic models of soil C storage were estimated (Fig. 3). This long-term k model
334 of soil C depletion in cropped soil had a reassuring coefficient of determination (R^2) of 90% and
335 a very low RMSEn of only 3.34%, which collectively indicates the high precision of the k
336 model. Over 250 years of cropland chronosequence, the C turnover rate was quantified as 0.010
337 $\pm 0.004 \text{ years}^{-1}$, which is equivalent to a MRT of 100 years and a half-life of soil C of 69 years.
338 This first-order trajectory of soil C depletion in croplands indicated that 28.9% of the initial soil
339 C under native grassland was gradually lost – i.e., very likely to the atmosphere – over 250 years
340 of annual cropping (i.e., from 1 to 0.711, Fig. 3). In further details, during the first year of
341 cropping, we estimated that 0.310% of the pre-existing C was lost from the soil. Conversely,
342 after 250 years, during the last year of the cropland-chronosequence trajectory, soil C losses were
343 only 0.026% of the initial soil C – this is one order of magnitude lower than calculated for the
344 first year of cropping. This deceleration in SOM mineralization while approaching a new
345 equilibrium and at near steady state was captured reasonably well by first-order kinetics. Based
346 on the soil C initially present under native grassland soils (3-chronosequence mean = 125.3 Mg C
347 ha^{-1} , Fig. 2), these values of 0.31% and 0.026% were equivalent to C outputs of 392 and 33 Kg C
348 $\text{ha}^{-1} \text{ yr}^{-1}$, respectively.

349 We projected two potential trajectories (A and B) of how afforested soils can restore soil
350 C storage in cropland soils over five decades (Fig. 3). Upon accounting for the replenishment of
351 81% of the soil C storage caused by shelterbelts (Table 1), we estimated that the afforested soils
352 reached a soil C storage of 94.5% (i.e., $0.81 \times 0.289 + 0.711 = 0.945$) relative to the soil C
353 present in the initial native grassland soils. Trajectory A was estimated on the basis that



354 afforested soils fully reached a new steady state and equilibrium of soil C storage with first-order
355 modelling. This trajectory showed a steep increase in soil C storage over the first decade of tree
356 planting. In fact, the C accretion rate for trajectory A was 0.119 years^{-1} , which suggests a
357 potential for high soil C accretion under fast C cycling with afforestation. Because the soils
358 beneath the shelterbelt can still be actively accruing C even 55 years after tree planting, we also
359 developed trajectory B, which targets a scenario where soil C storage reached 95% of a
360 theoretical equilibrium (Fig. 3). For this trajectory, the resultant C accretion rate was 0.0334
361 years^{-1} , which corresponds to a modelled MRT of 30 years. When focusing on these progressive
362 gains of new soil C under trajectory B, the estimated time for half of this soil C portion to enter
363 the soil was 21 years. Over the two last decades of this progression, the soil C accretion starts to
364 gradually become asymptotic. During the first year of trajectory B, the net accrual of soil C was
365 equivalent to 0.88% of the soil C initially present in the native grasslands (Fig. 3). Conversely,
366 during the last year of trajectory B, soil C accretion corresponded to only 0.17%. Based on the
367 soil C initially present under native grassland soils (3-chronosequence mean= $125.3 \text{ Mg C ha}^{-1}$,
368 Fig. 2), these 0.88% and 0.017% values were equivalent to a sizable 1.10 and $0.21 \text{ Mg C ha}^{-1} \text{ yr}^{-1}$,
369 respectively. It is noted that in each of the two afforestation trajectories of soil C accretion (A
370 and B), the annual contributions of afforestation to net accrual of soil C began from the soil C
371 storage estimated by the k-modelled cropland trajectory 50 years prior to soil sample collection
372 (i.e., 0.728 , Fig. 3). This is because we had assumed a lag phase of 5 years as noted above, and
373 tree planting was 55 years prior to soil sample collection.

374 Based on the assembled k models of cropland-C turnover and simultaneous tree-C
375 accretion (Fig. 3), of the whole soil C measured beneath the trees at the time of soil sample
376 collection (Table 1), 25% was estimated to be derived directly from tree-C contributions [i.e.,



377 (0.945 – 0.711) / 0.945]. This can indicate that although tree-C contributions were substantial,
378 the majority of the C stored in these steppe soils still originated from the initial native grassland
379 before land use conversion to annual croplands.

380 **3.2 Sources and turnover of soil C in afforested croplands: United States cases**

381 Larger accumulation of soil C was consistently found beneath trees relative to the
382 adjacent annual croplands in all three study sites within the Northern Great Plains of the United
383 States. At the shelterbelts in Norfolk (Fig. 4E) and Mead (data not shown) as well as the forest
384 plantation in Huron (Fig. 4F), tree-derived soil C were clearly discernable, in particular within
385 the 0 to 15 cm soil depth increment (Table 2).

386 At the Norfolk site, soils collected from the 0 to 15 cm depth increment beneath the trees
387 (i.e., within 10 m distance from the center of the shelterbelt) resulted in more than double of the
388 C mass density found in the annually-cropped topsoils that were located farthest from the trees
389 (28 vs. 13 Mg C ha⁻¹; Table 2, Fig. 4A). Concurrently, when comparing the same surface layer
390 and spatial sampling locations, soil δ¹³C sharply shifted from a considerably depleted -25.7 ± 0.1
391 ‰ beneath the trees to -17.5 ± 0.1 ‰ in the cropped soils north from the shelterbelt (Fig. 4C). As
392 a result, a significant 79% of the soil C storage measured beneath the trees at the time of sample
393 collection was attributed to tree-C contributions (Table 2). This translated into a substantial
394 magnitude of 22 Mg C ha⁻¹ being derived specifically from tree biomass (Table 2). Moreover, as
395 stated above (Method section 2.3), the rest of the soil C was attributed to remaining prairie-C.
396 The existing soil C beneath trees in the Norfolk shelterbelt allotted to remaining prairie-C was
397 only 45.5 ± 0.3 % of the whole soil C typically found in the adjacent annual crop field (Table 2).
398 This indicated that 54.5% of the soil C (equivalent to 13.0 - 5.9 = 7.1 ± 0.4 Mg C ha⁻¹, Table 2)
399 that existed under the long-term annual cropland (i.e., assumed to be at steady state) prior to tree



400 planting has been lost from the topsoil over the 70 years of afforestation at Norfolk. This net
401 decline in remaining prairie-C is attributable to CO₂ respiratory losses from enhanced biological
402 activity beneath the trees that gradually accessed, mobilized, cycled and partly mineralized this
403 legacy prairie-C pool. These results indicated that the turnover of remaining prairie-C in
404 afforested soils can be even faster than in open cropland fields.

405 Because the crop field south from the shelterbelt in Norfolk was dedicated to perennial
406 cropping of alfalfa forage – a C3 species, we undertook a mass balance to distinguish and
407 allocate the C sources as alfalfa-C vs. remaining prairie-C, with a similar approach as in the
408 afforested areas (i.e., Eq. [4] and [5]). Within the 0 to 15 cm depth increment, soil C storage
409 under alfalfa (i.e., 13.1 ± 1.0 Mg C ha⁻¹) was the same as in the annual cropland on the north side
410 of the shelterbelt (Fig. 4A; Table 2). However, the soil δ¹³C shifted to -21.6 ± 0.4 ‰, which
411 resulted in a 41.2 ± 0.4% replacement of the whole soil C storage being derived specifically from
412 recent contributions of alfalfa-C in this perennial forage field.

413 Similar to Norfolk, the shelterbelt at Mead also showed a major contribution of
414 afforestation to whole soil C storage between tree rows in the 0 to 15 cm depth increment (i.e.,
415 17 Mg C ha⁻¹, Table 2), which corresponded to 37% of the whole soil C. It is noted that although
416 the magnitude of original prairie-C lost after 35-yr of afforestation at Mead (i.e., 36.2 - 29.3 =
417 6.9 ± 0.7 Mg C ha⁻¹, Table 2) was comparable to Norfolk, the proportion of this original prairie-
418 C lost from afforested soils in Mead was much smaller with only 19% (i.e., 100 - 80.9; Table 2).
419 This can indicate that net changes in soil C storage under afforestation simultaneously
420 encompassing the noted prairie-C losses and the asymmetrically-larger tree-C gains followed a
421 stoichiometry of absolute capacities, instead of a proportionality of the initial prairie-C.



422 At the 19-year-old forest plantation at Huron, trees also increased soil C storage while
423 decreasing the $\delta^{13}\text{C}$ signature, in particular in the 0 to 15 cm depth increment (Fig. 4B, Fig. 4D).
424 When contrasting the afforested soils collected at least 17 m away from the plantation boundary
425 vs. topsoils taken within the adjacent cropland from the sampling locations that were farthest
426 removed from the trees, $\delta^{13}\text{C}$ changed from $-20.7 \pm 0.2 \text{ ‰}$ to $-17.3 \pm 0.1 \text{ ‰}$, respectively.
427 Although trees were much younger in Huron than in Mead and Norfolk, a considerable
428 magnitude of tree-C was found (i.e., 12 Mg C ha^{-1} , Table 2). This indicated that direct tree
429 contributions to soil C storage can take place rather quickly, within a few decades following
430 afforestation. However, the changes in the remaining prairie-C pool beneath the trees at Huron
431 apparently differed from what was found in both Mead and Norfolk. While soils beneath trees at
432 both Mead and Norfolk showed declines in remaining prairie-C relative to whole soil C stored in
433 open cropland fields at the time of sample collection, the afforested soil at Huron showed no
434 change in the magnitude of remaining prairie-C in the 0 to 15 cm depth increment. In fact, it is
435 striking how similar the whole C in the cropped soil ($25.6 \pm 0.7 \text{ Mg C ha}^{-1}$) was to the C
436 allocated to the remaining prairie-C pool beneath the trees ($25.3 \pm 0.7 \text{ Mg C ha}^{-1}$, Table 2). What
437 is more, the soils sampled from the adjacent native grassland within the Huron site also returned
438 a very consistent magnitude of soil C storage, with $25.4 \pm 1.9 \text{ Mg C ha}^{-1}$ ($n=3$, data not shown).
439 Provided the uncertainty of field sampling, this evidence strongly indicated that all or nearly all
440 the original prairie-C was retained and still present in the Huron soils under both annual cropping
441 and afforestation (Table 2). Likewise, when examining the 0 to 30 cm soil depth increment at
442 Huron (i.e., aggregating the two sampled soil layers shown in Fig. 4B), we further corroborated
443 this similarity in soil C storage between native grassland and annual cropland (45.4 ± 1.0 vs. 44.2
444 $\pm 1.1 \text{ Mg C ha}^{-1}$, respectively, data not shown)



445 Significant regressions revealed the consistent dependency of C source allocations on
446 time since tree planting (Fig. 5). Over time following afforestation, tree-C source increased
447 linearly from an assumed null contribution at planting to become 79% of the whole soil C after
448 70 years of tree planting in Norfolk ($R^2= 0.95$, Fig. 5A). We also evaluated changes over time for
449 the remaining prairie-C in afforested soils relative to the corresponding adjacent croplands within
450 each study site. Linearity of these prairie-C proportions as a function of time was also observed
451 when encompassing the three study sites ($R^2= 0.999$, Fig. 5B). As described above, the more
452 recently-afforested soils at the Huron site kept the entire prairie-C, while the oldest afforested
453 soils at the Norfolk site retained less than half of the whole soil C present in the adjacent annual
454 croplands (45.5%).

455 We focused on estimating the turnover rates of soil C mass density derived directly from
456 tree-C sources while encompassing the range of conditions in the three study studies. As most of
457 the beneficial effects of tree planting across the sites in the United States were detected in the 0
458 to 15 cm soil depth increment, further examination of accretion rates of soil C storage focused on
459 this specific topsoil layer. Upon assembling the magnitudes of tree-C contributions over time
460 since afforestation, unified first-order kinetics modelling converged and emerged robustly ($R^2=$
461 0.997 , Fig. 6). The k rate constant of $0.0552 \text{ years}^{-1}$ corresponds to a half-life of 12.6 years,
462 which indicates that more than half of the accrual tree-C occurred within less than two decades
463 (when accounting for a lag phase of 5 years following tree planting) (Fig. 6). This further
464 substantiated the rapid contributions of afforestation to increase soil C storage quickly until
465 reaching a new dynamic equilibrium. This generalized relationship enabled projecting tree-C
466 accruals in afforested soils within the assessed time range of 70 years. We further implemented
467 this robust k -progression to simultaneously depict the gains in tree-C while also representing the



468 declines in prairie-C in afforested soils for each study site separately (Fig. 7). This approach
469 accounts for the C that is being lost from net mineralization of pre-existing C in the remaining
470 prairie SOM (Fig. 7). It was noticeable that the afforested soils at Mead showed faster turnover
471 rate of the remaining prairie-C than the other two sites by approximately two-fold. The k rate
472 constant of net mineralization of prairie-C beneath trees at Mead was 0.145 years^{-1} (Fig. 7B),
473 which corresponded to an MRT of about 7 years. This implies that the average time for prairie-C
474 to be lost from Mead afforested soils was well within one decade, whereas prairie-C in afforested
475 soils in Huron and Norfolk showed longer residence times by about double.

476

477 **4 Discussion**

478 **4.1 Carbon contributions from trees to SOM sequestration**

479 Planting trees in croplands creates substantial sinks of atmospheric C in the soil profile
480 (Sauer et al., 2007; Khaleel et al., 2020; Zhang et al., 2020). Current knowledge of this important
481 benefit of afforestation has been deepened and reinforced earlier literature (Post and Kwon,
482 2000; Hernandez-Ramirez et al., 2011; Chendev et al., 2015b). It is noticeable that having long-
483 term annual croplands as the land use system prior to establishing trees particularly enlarges the
484 soil C sink and replenishment caused by afforestation (Guo and Gifford, 2002; Laganier et al.,
485 2010; Sauer et al., 2012). Overall results indicate that across tree species and local edaphic-
486 climatic conditions at the studied sites, the massive tree-C contributions through decaying roots
487 and litter (Li et al., 2012; Amadi et al., 2016) can saturate the soil with C substrates in surplus to
488 the capacity of microbial decomposition (Li et al., 2018; Deng et al., 2014), which collectively
489 incline the C balance towards net C accrual (Hernandez-Ramirez et al., 2011). Our quantification
490 of these tree biomass-C contributions to newly-accrued soil C further expand this growing body



491 of knowledge. The proportion of new soil C originated from tree biomass were shown to increase
492 significantly with time (Fig. 5A). As abovementioned, the shift from C4-dominated to C3
493 vegetation in the case of the afforested soils in United States enabled us to methodologically
494 apportion the sources of soil C and to identify these direct contributions from trees to increasing
495 soil C storage. In the case of the Russian sites, soil ^{13}C isotope composition does not resolve
496 these C sources because of the lack of shift between C4 and C3 vegetation in the natural history
497 of these landscapes.

498 By contrast to afforestation, long-term annual cropping implies recurrent soil mixing,
499 disruption of any preexistent vertical stratification, microclimate fluctuation, and exposure of
500 SOM to decomposition, which collectively shift the C balance and predispose towards depletion
501 of soil C (Post and Kwon, 2000; Hernandez-Ramirez et al., 2009; Curtin et al., 2014). In addition
502 to this disturbance and exposure of SOM to decomposition, low C inputs and high C removals
503 via harvest are also characteristic of conventional annual cropping systems. A reduction of C
504 inputs in croplands once the native vegetation (roots and aboveground biomass) have been
505 removed (Hu et al. 2013) is also typically followed by alterations in soil physical properties such
506 as decreases in porosity and gas exchange which can become detrimental to plant primary
507 productivity and soil biology (Kiani et al., 2017).

508 Our study explicitly examined and quantified for first time in literature the losses of
509 remaining prairie-C directly beneath trees across afforested soils (Fig. 3, Fig. 5B, Fig. 7). This
510 analyses showed that under afforestation, soil C remaining from original native grasslands
511 continues to be lost from the profile (Fig. 3, Fig. 7), likely via microbial mineralization. This
512 noted decline in remaining prairie-C beneath young afforestation agrees well with a rapid
513 decomposition of SOM in the early stage of tree growth as previously deliberated by Paul et al.



514 (2002), Garten (2002), and Xiong et al. (2020). At the Norfolk site, tree-C contributions
515 effectively replenished and greatly surpassed the gradual losses of remaining prairie-C in the soil
516 (Fig. 7C). In the case of Huron site, trees generated the conservation of the entire prairie-C
517 legacy while also contributing directly to additional tree-C accrued in an overall increasing SOM
518 pool (Fig. 7A).

519 It is noted that although the three US sites (Norfolk, Huron and Mead) shared a common
520 trajectory of tree-C accretion with time (Fig. 5, Fig. 6), their k turnover rates of remaining
521 prairie-C differed (Fig. 7). These apparent divergences are potentially attributable to differences
522 in temperature and moisture regimes across the region. In further details, in the case of accretion
523 of tree-C in afforested soils, this response to land use change seems governed mostly by the
524 change into tree vegetation and the duration of afforestation; therefore, it became feasible for us
525 to establish a unified, robust k model across a range of afforestation ages (Fig. 6). Conversely,
526 loss rates of remaining prairie-C in afforested soils appeared to be mostly contextual and even
527 site specific, likely as a function of local hydrothermal conditions (Chendev et al. 2014, 2015b).
528 Relative to both Norfolk and Huron (Fig. 7), warmer-wetter conditions in Mead could have led
529 to the faster C turnover rate and mineralization of the remaining prairie-C in these afforested
530 soils (Fig. 7B). Overall, these results exemplify how analyzing the compartments of soil C
531 turnover – evaluating separately tree-C contributions and remaining prairie-C, instead of
532 studying only the whole soil C – can provide further insights into SOM dynamics following land
533 use conversions. Future research could address the potential existence of underlying thresholds
534 of heat and moisture availabilities that are conducive to retain and converse pre-existing prairie-
535 C in afforested soils while simultaneously enabling soil C accretion directly from new tree-C
536 contributions.



537 Based on the kinetics-modelled reconstruction of soil C storage over time in the Russian
538 land use chronosequences (i.e., encompassing a range of different duration of cropping since
539 land use conversion), over the 55 years that elapsed since tree planting until soil sample
540 collection, the remaining soil C from the original native grassland was shown to continually
541 being lost (Fig. 3). Our turnover estimations using kinetics modelling suggested that only 1.7%
542 of the initial grassland-C was lost over these 55 years following shelterbelt afforestation (Fig. 3).
543 Mellor et al. (2013) stated that mycorrhizae development in afforested soils can preferentially
544 access and utilized remaining prairie-C beneath trees. This biological effect could contribute to
545 decreases in remaining prairie-C in afforested soils.

546 Chendev et al. (2014, 2015b) further addressed differences in soil C accrual across
547 afforested sites in Russia and the United States, also attributing them primarily to differences in
548 moisture regimes. Within each geographic region as well as in the collective of both countries,
549 they explained that cooler-moister conditions led to increases in overall soil C accrual beneath
550 trees. This postulate is clearly in line with earlier results by Garten (2002). Potential increases in
551 plant primary productivity with increasing moisture as well as reductions in microbial
552 mineralization of the overall SOM with colder conditions can shift and drive the C balance in the
553 soil towards net C accrual.

554 Of the three paired sites in Russia (Table 1), the Yamskaya site is probably the most
555 representative and closely related to the three long-term chronosequences evaluated in this study.
556 This is because Yamskaya and the three chronosequences are all geographically located within
557 the Belgorod oblast, and hence, they share a more similar regional hydrothermal regime. It was
558 striking that the afforested soil at Yamskaya site had a soil C accretion even greater than the
559 native grassland reference, which strongly indicated the high capacity of shelterbelts to sequester



560 C even beyond the capacity of the corresponding native ecosystem (Table 1). After noticing this
561 finding, it can also be anticipated that although the drier Kamennaya site showed at the present
562 the slowest soil C accretion following afforestation of SOM-depleted croplands (Table 1), it is
563 possible that in the long term, this drier environment can gradually sequestered even more soil C
564 than the moist sites located in Belgorod oblast (e.g., Yamskaya). This is suggested as the
565 Kamennaya site exhibited the highest soil C storage when comparing across all the native
566 grasslands compiled in our study (i.e., 152.5 Mg C ha⁻¹; Table 1 and Fig. 2).

567 **4.2 Turnover rates of soil carbon as a function of land use changes**

568 This study clearly confirms that the long-term dynamics of soil C is consistently
569 nonlinear, either during decline or accumulation of soil C as a function of land use choices. As
570 deliberated earlier by Post and Kwon (2000) and Garten (2002), erroneously assuming linearity
571 in depicting these trajectories of soil C would lead to underestimating the rates of soil C changes
572 during the first decades following a land use conversion as well as overestimating the turnover
573 rates of soil C after multiple decades once the ecosystem has actually reached stability and a
574 balance between their C inputs and outputs. This latter notion essentially applies when long-term
575 cropland or afforested fields have become mature (Hernandez-Ramirez et al., 2011)

576 Earlier chronosequence and stable isotope analyses by Arrouays et al. (1995) in
577 Southwest France further support that land use effects on soil C changes take place rather
578 quickly. They reported that a new equilibrium in soil C storage was reached within only few
579 decades of a land use change from forest to annual croplands, and with about half of the C loss
580 occurring rapidly within few years (< 10) of beginning cultivation (Arrouays et al., 1995).
581 Similarly, as in our study, only a few decades seems to be required to reach equilibrium when
582 switching from cropland to trees (Richter et al., 1999; Paul et al., 2002; Guo and Gifford, 2002).



583 Likewise, comprehensive results by Dhillon and Van Rees (2017) depicting soil C accretion
584 caused by afforestation in the Canadian Prairies can be interpreted as net C losses taking place
585 over the first several years after tree planting, and subsequently, an ensuing fast accrual of soil C
586 until tree ages of about 35 years when new equilibria or C sequestration ceilings under
587 afforestation can be reached. In our study, MRT of soil C accretion beneath trees were in general
588 determined to be about two decades (Fig. 6). Furthermore, the evaluation of our two scenarios of
589 asymptotic equilibria of C accrual in afforested soils (i.e., trajectories A and B in the normalized
590 Russian chronosequences; Fig. 3) can provide the boundaries of faster vs. slower C accretion
591 with MRTs of one vs. three decades, respectively.

592 In the case of long-term annual croplands in Russia, the MRT of 100 years for soil C
593 depletion found in our study (i.e., associated with a k rate constant of 0.010 years^{-1} , Fig. 3) is
594 comparable to findings by Huggins et al. (1998) who registered MRTs of 91 and 143 years in
595 annual cropping systems in Minnesota, but overall longer than a report by Collins et al. (1999)
596 who found a wide range of MRTs between 18 to 96 years for sites with 8 to 33 year-old
597 continuous maize cropping across the Central United States, respectively.

598 It is noted that the exponential first-order trajectory of soil C turnover in the Russian
599 chronosequences (Fig. 3) was captured better with Eq. [1] than the simplistic $C_{(t)} = C_0 \times e^{-kt}$
600 previously used by Hernandez-Ramirez et al. (2011). While Eq. [1] provided an R^2 of 90% (Fig.
601 3), $C_{(t)} = C_0 \times e^{-kt}$ returned an R^2 of 68% (data not shown). With two fitting parameters (i.e., C_0 ,
602 C_e), first-order kinetic modelling with Eq. [1] represented reasonably well the assumptions of
603 steady state and new equilibrium at the end of the evaluated time series (Fig. 3, Fig. 6).

604 Further kinetics modelling efforts of soil C increases in afforested systems can take the
605 form of two functional C pools where inputs and outputs to labile and recalcitrant SOM can be



606 predicted (Arrouays et al., 1995; Garten, 2002; Hernandez-Ramirez et al., 2009; Xiong et al.,
607 2020). Preferentially accruing C into recalcitrant vs. labile SOM pools in afforested soils can be
608 interpreted as tree-C contributions towards long- vs. short-term stability of soil C storage,
609 respectively, with crucial ramifications for mitigation of future climate change (Laganiere et al.,
610 2010; Hernandez-Ramirez et al., 2011; Deng et al., 2014). Future investigations can also focus
611 on the protection and stabilization mechanisms of SOM as created by soil aggregate formation
612 beneath trees (Kiani et al., 2017; Quesada et al., 2020). Once soils subjected to long-term annual
613 cropping are converted to permanent vegetation, fungal hyphae can become an important means
614 that mediates C accretion by enhancing soil aggregation (Jastrow et al., 1996; Kiani et al., 2017).
615 Jastrow et al. (1996) indicated that fungal hyphae could improve macroaggregation and hence
616 indirectly enhance C accrual. Using phospholipid fatty acid biomarkers, Kiani et al. (2017)
617 identified a linkage between presence of fungal biomass and increases in hierarchical fractal
618 aggregation specifically in forest soils, while this association was absent in the adjacent
619 annually-cropped soils in their study. Furthermore, Quesada et al. (2020) recently discussed the
620 mechanisms for soil C accretion in tropical forests. In line with earlier findings by Wang et al.
621 (2016), Quesada et al. (2020) stated that SOM physical protection provided by the formation of
622 soil aggregates slows decomposition of SOM within aggregates, and hence, it becomes a second
623 layer of stabilization after realizing the primary SOM stabilizing effects caused by mineral
624 surfaces of fine soil particles such as silt and clay. Further studies can focus on the effects of
625 inherent mineralogy and texture as well as clay leaching processes on C dynamics and storage in
626 afforested soils (Chendev et al., 2020; Quesada et al., 2020).

627

628 **5 Summary**



629 Nonlinear turnover rates of soil C revealed an MRT of a century in long-term croplands
630 as soil C slowly undergoes depletion and losses to the atmosphere. Likewise, when croplands
631 were afforested, nonlinear accretion rates of soil C indicated a MRT of approximately two
632 decades following afforestation. Soil C showed to be rapidly accrued as trees remove CO₂ from
633 the atmosphere and contribute C substrates for SOM accumulation and stabilization. Results
634 collectively substantiated that in addition to other important benefits by trees such as providing
635 air quality, microclimate regulation and erosion control (Sauer et al., 2007; Hernandez-Ramirez
636 et al., 2012), C sequestration in afforested lands is a suitable means to proactively address and
637 effectively mitigate ongoing climate change within a person's lifetime.

638



639 **Data availability**

640 Data are available on request.

641

642 **Author contribution**

643 GHR: Conceptualization; Methodology; Formal analysis; Funding acquisition; Resources;

644 Visualization; Writing the original draft; Review and editing new versions; Corresponding

645 author role.

646 TJS and YGC: Conceptualization; Data curation; Formal analysis; Funding acquisition;

647 Investigation; Methodology; Supervision; Project administration; Resources; Visualization;

648 Review and editing new versions.

649 ANG: Investigation; Methodology; Funding acquisition; Review and editing new versions.

650

651 **Competing interests.**

652 The authors declare that they have no conflict of interest.

653

654 **Acknowledgement**

655 The authors are grateful for the valuable assistance provided by Kent Heikens, Kevin Jensen,

656 David Denhaan, and Amy Morrow. The first author acknowledges early encouragements and

657 beneficial exchange of ideas on the study subject with Dr. Cindy A. Cambardella – now

658 deceased. We sincerely appreciate the funding support as follows: from Natural Sciences and

659 Engineering Research Council of Canada (NSERC) Discovery program (Canada) as well as

660 Alexander von Humboldt Foundation (Germany) to GHR; from U.S. Civilian Research and

661 Development Foundation - Cooperative Grants Program (Project RUG1-7024-BL-11) to TJS and



662 YGC; and from Russian Science Foundation (Project 19-17-00056) for field sample collection

663 and laboratory analyses within Russian sites to YGC and ANG.

664



665 **References**

- 666 Amadi, C.C., Van Rees, K.C.J., and Farrell, R.E. 2016. Greenhouse gas mitigation potential of
667 shelterbelts: Estimating farm-scale emission reductions using the Holos model. *Canadian*
668 *Journal of Soil Science*, 97(3): 353-367
- 669 Arrouays, D., Balesdent, J., Mariotti, A., Girardin, C., 1995. Modelling organic carbon turnover
670 in cleared temperate forest soils converted to maize cropping by using ^{13}C natural
671 abundance measurements. *Plant Soil* 173, 191 – 196.
- 672 Chendev, YG, AN Gennadiev, SV Lukin, TJ Sauer, EA Zazdravnykh, VG Belevantsev, MA
673 Smirnova. 2020. Change of Forest-Steppe Chernozems under the Influence of
674 Shelterbelts in the South of the Central Russian Upland. *Eurasian Soil Science*, Volume
675 53, Issue 8, p.1033-1045
- 676 Chendev, YG, CL Burras, TJ Sauer. 2012. Transformation of forest soils in Iowa (United States)
677 under the impact of long-term agricultural development. *Eurasian Soil Science* 45:357-
678 367.
- 679 Chendev, YG, LL Novykh, TJ Sauer, AN Petin, EA Zazdravnykh, CL Burras. 2014. Evolution
680 of soil carbon storage and morphometric properties of afforested soils in the US Great
681 Plains. *Soil Carbon*, 475-482
- 682 Chendev, YG, TJ Sauer, AN Gennadiev, LL Novykh, AN Petin, VI Petina. 2015a. Accumulation
683 of organic carbon in chernozems (Mollisols) under shelterbelts in Russia and the United
684 States. *Eurasian soil science* 48 (1), 43-53
- 685 Chendev, YG, TJ Sauer, G Hernandez-Ramirez, CL Burras. 2015b. History of East European
686 chernozem soil degradation; protection and restoration by tree windbreaks in the Russian
687 steppe. *Sustainability* 7 (1), 705-724



- 688 Curtin, D, Beare MH, Scott CL, Hernandez-Ramirez, G. and Meenken ED. (2014).
689 Mineralization of soil carbon and nitrogen following physical disturbance: a laboratory
690 assessment. *Soil Sci. Soc. Am. J.* 78: 925–935
- 691 Deng, Q., X. Cheng, Y. Yang, Q. Zhang, Y. Luo. 2014. Carbon-nitrogen interactions during
692 afforestation in central China. *Soil Biol. Biochem.*, 69:119-122
- 693 Dhillon, G.S., and K.C.J. Van Rees. 2017. Soil organic carbon sequestration by shelterbelt
694 agroforestry systems in Saskatchewan. *Can. J. Soil Sci.* 10.1139/CJSS-2016-0094
- 695 Follett, R., E. Paul, S. Leavitt, A. Halvorson, D. Lyon and G. Peterson. 1997. Carbon isotope
696 ratios of Great Plains soils and in wheat-fallow systems. *Soil Sci. Soc. Am. J.* 61:1068-
697 1077.
- 698 Garten, C.T. 2002. Soil carbon storage beneath recently established tree plantations in Tennessee
699 and South Carolina, USA. *Biomass Bioenergy* 23:93–102.
- 700 Guenette, K.G. and G. Hernandez-Ramirez. 2018. Tracking the influence of controlled traffic
701 regimes on field scale soil variability and geospatial modeling techniques. *Geoderma*
702 328:66-78.
- 703 Guo, LB, Gifford RM (2002) Soil carbon stocks and land use change: a meta analysis. *Global*
704 *Change Biology*, 8, 345–360.
- 705 Hebb, C, Schoderbek D, Hernandez-Ramirez, G., Hewins D, Carlyle CN, Bork E. (2017). Soil
706 physical quality varies among contrasting land uses in Northern Prairie regions. *Agric.*
707 *Ecosyst. Environ.* 240:14–23.
- 708 Hernandez-Ramirez, G., Brouder, S.M., D.R. Smith, and G.E. Van Scoyoc. (2009) Carbon and
709 nitrogen dynamics in an Eastern Corn Belt soil: N source and rotation. *Soil Sci. Soc. Am.*
710 *J.* 73:128-137



- 711 Hernandez-Ramirez, G., Sauer, T.J., C.A. Cambardella, J.R. Brandle, and D.E. James. (2011)
712 Carbon sources and dynamics in afforested and cultivated corn belt soils. *Soil Sci. Soc.*
713 *Am. J.* 75:216–225
- 714 Hernandez-Ramirez, G., Trabue SL, Sauer TJ, Pfeiffer RL, Tyndall JC. (2012). Odor mitigation
715 with tree buffers: swine production case study. *Agric. Ecosyst. Environ.* 149:154–163.
- 716 Hu, Y., D. Zeng, S. Chang, R. Mao. 2013. Dynamics of soil and root C stocks following
717 afforestation of croplands with poplars in a semi-arid region in northeast China. *Plant*
718 *Soil*, 368:619-627
- 719 Khaleel, A.A., TJ Sauer, JC Tyndall. 2020. Changes in deep soil organic carbon and soil
720 properties beneath tree windbreak plantings in the US Great Plains. *Agroforestry*
721 *Systems*, 1-17
- 722 Kiani, M, Hernandez-Ramirez, G., Quideau S, Smith E, Janzen H, Larney F, Puurveen D.
723 (2017). Quantifying sensitive soil quality indicators across contrasting long-term land
724 management systems: crop rotations and nutrient regimes. *Agric. Ecosyst. Environ.*
725 248:123–135.
- 726 Kiani, M., G. Hernandez-Ramirez and S.A. Quideau. In press. Spatial variation of soil quality
727 indicators as a function of land use and topography. *Can. J. Soil Sci.* 1-16.
- 728 Laganiere, J., D.A. Angers, D. Pare. 2010. Carbon accumulation in agricultural soils after
729 afforestation: a meta-analysis. *Global Change Biology*, 16 (1) 439-453
- 730 Li, D., S. Niu and Y. Luo. 2012. Global patterns of the dynamics of soil carbon and nitrogen
731 stocks following afforestation: A meta-analysis. *New Phytol.* 195:172-181.



- 732 Li, J.C., Hernandez-Ramirez, G., Kiani, M., Quideau, S., Smith, E., Janzen, H., Larney, F., Puurveen,
733 D (2018). Soil organic matter dynamics in long-term temperate agroecosystems: rotation
734 and nutrient addition effects. *Canadian Journal of Soil Science*, 98, 232-245
- 735 Martin, A., Mariotti A, Balesdent J, Lavelle P and Vuattoux R. 1990. Estimate of organic matter
736 turnover rate in a savannah soil by ^{13}C natural abundance. *Soil Biol. Biochem.* 22, 517-
737 523.
- 738 Mellor, N.J., J. Hellerich, R. Drijber, S.J. Morris, M.E. Stromberger and E.A. Paul. 2013.
739 Changes in ecosystem carbon following afforestation of native sand prairie. *Soil Sci. Soc.*
740 *Am. J.* 77:1613-1624.
- 741 Parry, M., Parry, M. L., Canziani, O., Palutikof, J., Van der Linden, P., and Hanson, C. (2007).
742 Climate change 2007-impacts, adaptation and vulnerability: Working group II
743 contribution to the fourth assessment report of the IPCC. Cambridge University Press,
744 Cambridge, United Kingdom
- 745 Paul, K.I., Polglase P.J., Nyakuengama J.G., Khanna P.K. (2002) Change in soil carbon following
746 afforestation. *Forest Ecol Manag* 168:241–257
- 747 Post, W.M., and K.C. Kwon. 2000. Soil carbon sequestration and land-use change: processes and
748 potential. *Global Change Biology*, 6:317-327
- 749 Quesada, C. A., Paz, C., Oblitas Mendoza, E., Phillips, O. L., Saiz, G., and Lloyd, J.: Variations
750 in soil chemical and physical properties explain basin-wide Amazon forest soil carbon
751 concentrations, *SOIL*, 6, 53–88, <https://doi.org/10.5194/soil-6-53-2020>, 2020.
- 752 Richter, D.D., D. Markewitz, S.A. Trumbore, and C.G. Wells. 1999. Rapid accumulation and
753 turnover of soil carbon in a re-establishing forest. *Nature* 400:56–58.



- 754 Sauer, T.J., C.A. Cambardella, and J.R. Brandle. 2007. Soil carbon and tree litter dynamics in a
755 red cedar–Scotch pine shelterbelt. *Agrofor. Syst.* 71:163–174.
- 756 Sauer, TJ, DE James, CA Cambardella, G Hernandez-Ramirez. 2012. Soil properties following
757 reforestation or afforestation of marginal cropland. *Plant and soil* 360 (1-2), 375-390
- 758 Thilakarathna, S. K., and Hernandez-Ramirez, G. (in press). "How does Management Legacy,
759 Nitrogen Addition and Nitrification Inhibition Impact Soil Organic Matter Priming and
760 Nitrous Oxide Production?" *Journal of Environmental Quality*, doi: 10.1002/jeq2.20168
- 761 Wang, F., W. Zhu, H. Chen. 2016. Changes of soil C stocks and stability after 70-year
762 afforestation in the Northeast USA. *Plant Soil*, 401: 319-329, 10.1007/s11104-015-2755-
763 3
- 764 Xiong, X., H.L. Zhang, Q. Deng, D.F. Hui, G.W. Chu, Z. Meng, G.Y. Zhou, D.Q. Zhang. 2020.
765 Soil organic carbon turnover following forest restoration in south China: Evidence from
766 carbon isotopes. *Forest Ecol. Manag.*, 462: 117988
- 767 Zhang, Q.Y., X.X. Jia, X.R. Wei, M.A. Shao, T.C. Li, Q. Yu. 2020. Total soil organic carbon
768 increases but becomes more labile after afforestation in China's Loess Plateau. *For. Ecol.*
769 *Manag.* 461 (2020), Article 117911, 10.1016/j.foreco.2020.117911
- 770



Table 1. Soil organic carbon storages and differences within the 0 to 30 cm depth increment under three land uses (i.e., native grasslands, annual croplands and afforestation) in Russia. The nine values of soil C storage across the nine site-land uses were previously presented and discussed in Chendev et al. (2015b) and are repeated here for informing first-order kinetic modelling and estimations of C accretion rates when converting from annual croplands to afforestation as shown in Fig. 3.

Land use or descriptor	Streletskaya Steppe site, Kursk	Yamskaya Steppe site, Belgorod	Kamennaya Steppe site, Voronezh	3-sites mean	Standard error
Soil C mass density (Mg C ha ⁻¹)					
Native grassland (G)	126.2	138.0	152.5	138.9	7.61
Annual cropland (C)	109.3	127.2	123.6	120.0	5.47
Shelterbelt (Trees)	126.4	142.1	125.0	131.2	5.48
Net decrease G-to-C	-16.9	-10.8	-28.9	-18.9	5.32
Net increase C-to-Trees	17.1	14.9	1.40	11.1	4.91
G-to-C / C-to-Trees [†]	1.01	1.38	0.05	0.81	0.40

[†]Ratio representing the replenishing of depleted soil C by tree planting. These ratios were calculated as the absolute values of net increase from cropland to shelterbelt (trees) divided by net decrease from grassland to cropland.



Table 2. Soil organic carbon storage within the 0 to 15 cm depth increment contrasting annual croplands and afforestation in United States. Sources of soil C storage beneath the trees were allocated as tree-C versus remaining prairie-C using Eq. [4] and [5] and associated assumptions. Error bars are standard errors of the means.

Site	Tree age (years)	Whole soil C mass density		Tree-C contribution to soil C		Remaining prairie-C		Remaining prairie-C / whole C in cropland [†]
		Annual cropland (Mg C ha ⁻¹)	Beneath trees (Mg C ha ⁻¹)	Mass density (Mg C ha ⁻¹)	Proportion (%)	Mass density (Mg C ha ⁻¹)	Proportion (%)	Proportion (%)
Huron, S. Dakota	19	25.6 ± 0.7	37.5 ± 1.2	12.2 ± 0.8	32.6 ± 1.5	25.3 ± 0.7	67.4 ± 1.5	98.8 ± 2.8
Mead, Nebraska	35	36.2 ± 0.4	46.7 ± 1.5	17.4 ± 1.2	37.2 ± 1.8	29.3 ± 1.9	62.8 ± 1.8	80.9 ± 3.6
Norfolk, Nebraska	70	13.0 ± 1.3	28.0 ± 1.4	22.1 ± 1.1	78.9 ± 1.0	5.90 ± 0.42	21.1 ± 1.0	45.5 ± 0.3

[†] This ratio represents the proportion of remaining prairie-C relative to whole soil C in annual cropland. The magnitudes of both ‘remaining prairie-C’ and ‘whole soil C in annual cropland’ are shown in other columns of this same table. It is noted that balance (e.g. in Mead, 100 - 81 = 19) represents to the proportion of prairie-C lost in afforested soils since tree planting.

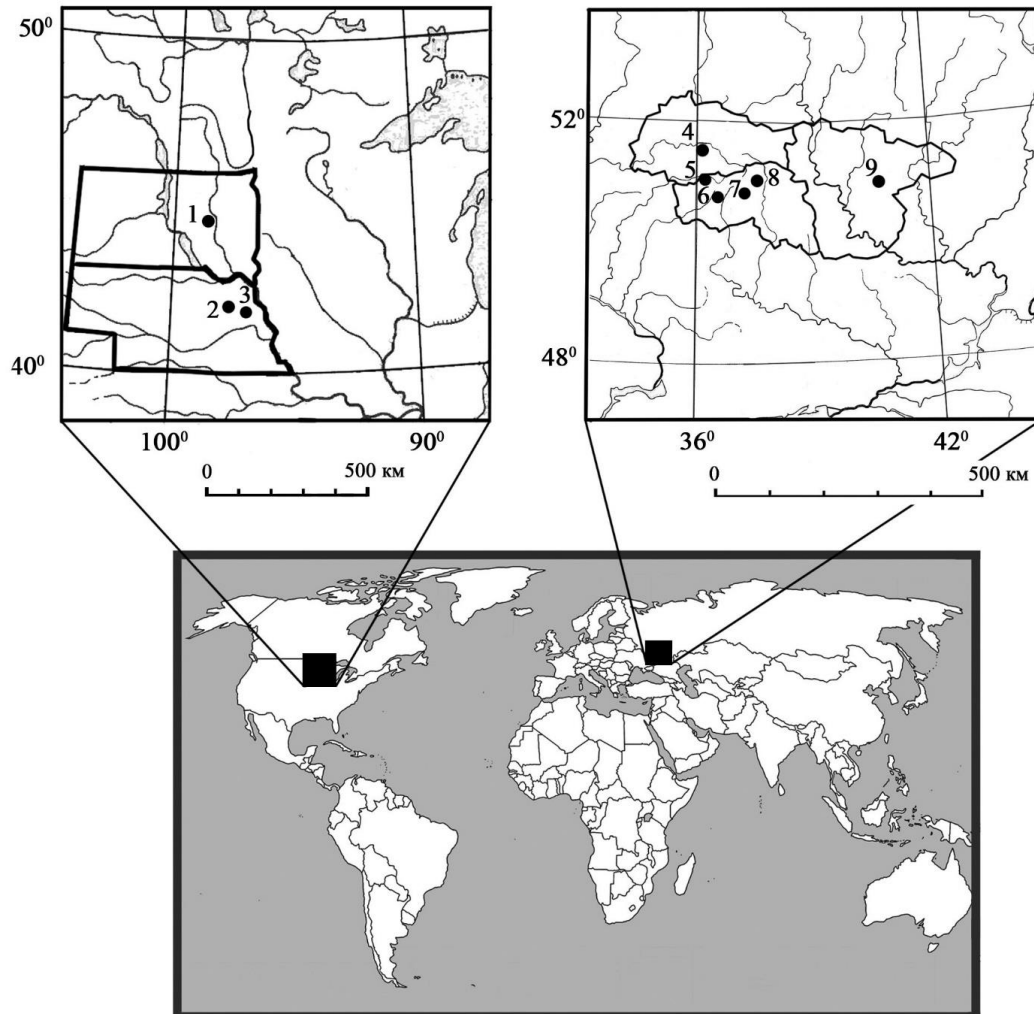


Fig. 1. Geographical location of the nine study sites within the United States (1. Huron, 2. Norfolk, 3. Mead) and Russia (4. Streletsкая Steppe, 5. Ivnyanskiy, 6. Prokhorovskiy, 7. Gubkinskiy, 8. Yamskaya Steppe, 9. Kamennaya Steppe). Within Russia, 5, 6, and 7 are sites with chronosequences of land use conversion, while 4, 8 and 9 are paired sites (native grasslands, annual croplands versus shelterbelts). The three sites in the United States are paired sites (afforestation vs. adjacent annual croplands).

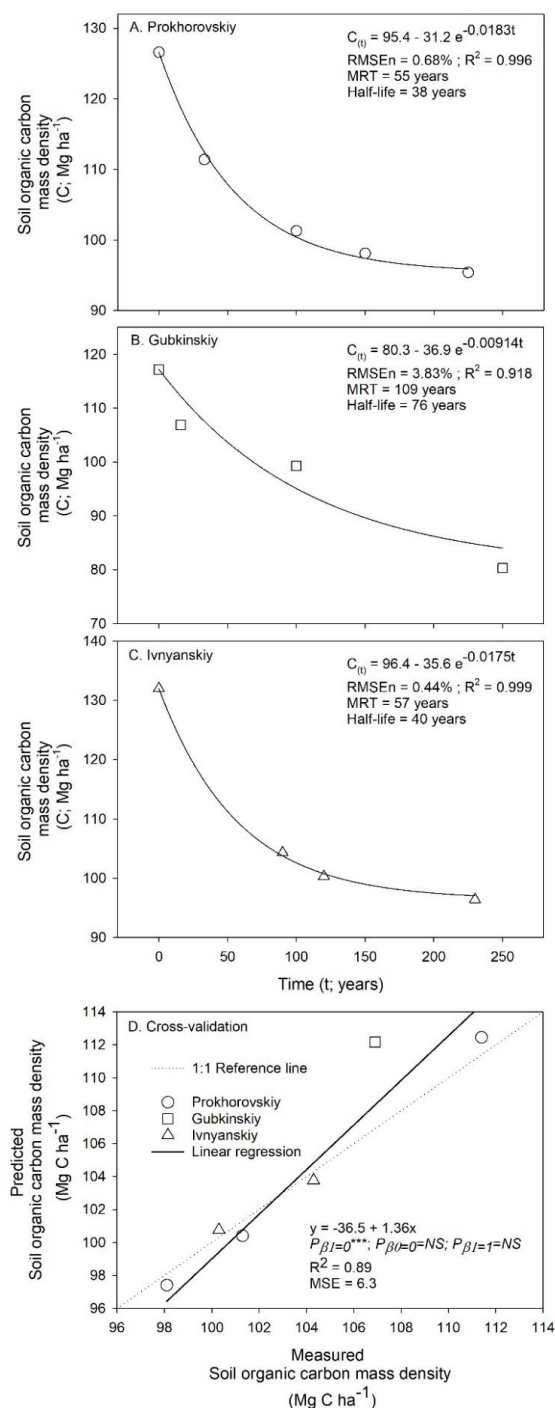


Fig. 2. Land use chronosequences of soil organic carbon storage within the 0 to 30 cm depth increment after converting native grassland to annual croplands in Belgorod oblast, Russia. These showed soil C declines over time. (A) Prokhorovskiy, (B) Gubkinskiy and (C) Ivnyanskiy districts. In Panels A, B and C, first-order kinetic models are described by the solid curvilinear fittings and equations in the form $C_{(t)} = C_e + (C_0 - C_e) e^{-kt}$ where C_e is C at new dynamic equilibrium (inputs = outputs), C_0 is initial C at time of land use conversion (time zero), k is the first-order kinetic rate constant equivalent to turnover rate. As reciprocal of k , MRT stands for mean residence time, while half-life equates to $\ln(2)/k$. Normalized root mean square error (RMSEn) and coefficient of determination (R^2) for each k model are provided. (D) Cross-validation of first-order predicted C versus measured C encompassing the three chronosequences within the age range from 10 to 200 years. Mean squared error (MSE) and R^2 for the cross-validation are provided. The subscripts of the P values denote the null hypotheses for testing the regression coefficient (β_1) and intercept (β_0), where $***$ is a p -value of <0.001 and NS is non-significant. First-order kinetic modelling was supported by this performance evaluation.

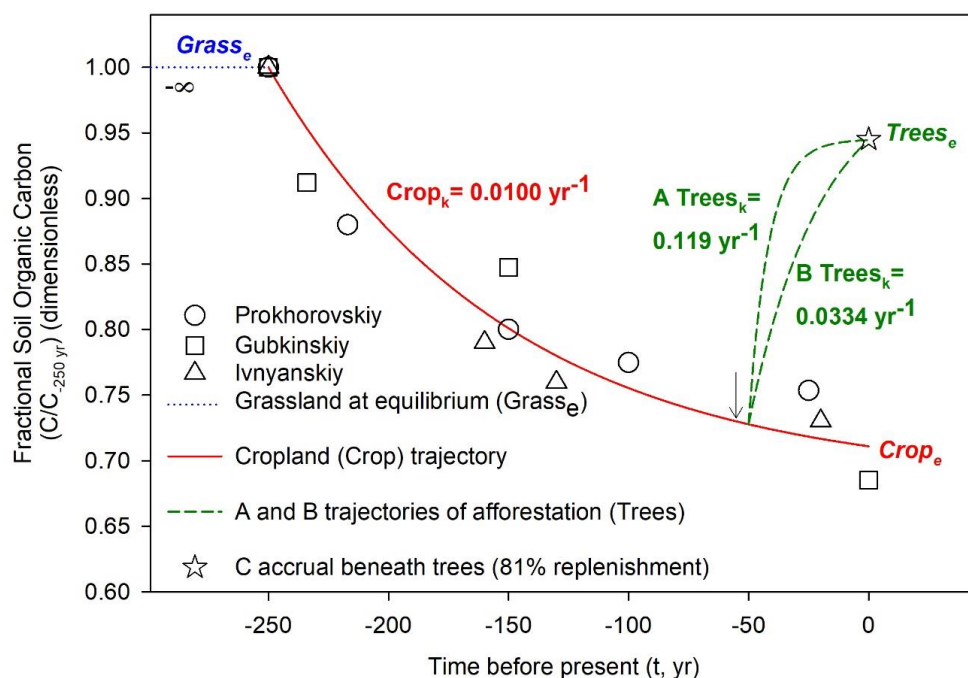


Fig. 3. Reconstruction of soil organic carbon storage within the 0 to 30 cm depth increment following land use conversions from native grassland to annual cropland and subsequently into afforestation with shelterbelts in Russia. This assemblage assumed that native grasslands were at dynamic equilibrium and steady state prior to conversion to annual croplands. Likewise, nonlinear k estimates of turnover rates in croplands and accretion rates under afforestation also required the assumptions of reaching new dynamic equilibria and steady state at zero year (i.e., time of soil sample collection). The cropland trajectory of soil C over time was derived from chronosequence data presented in Fig. 2A, Fig. 2B and Fig. 2C. The soil C accrual beneath trees at time zero (open star) was estimated from measured data presented in Table 1 (i.e., of the soil C that had been depleted by cropping, afforestation replenished 81%, based on 3-sites mean). Note that although trees were planted on year -55 (vertical arrow ↓), tree-C contributions to soil C accrual were accounted for starting from year -50 based on a literature review by Paul et al. (2002) that suggested a lag phase of 5 years. The trajectory ‘B Trees’ (dashed red line with $k = 0.0334 \text{ yrs}^{-1}$) assumed that the soil C storage had asymptotically reached 95% of a theoretical equilibrium (i.e., ‘Trees_e’ / 0.95). First-order kinetic modelling was used to derive these three nonlinear trajectories of soil C with the general form $C(t) = C_e + (C_o - C_e) e^{-kt}$. With the aim of integrating information from the three available chronosequences (Fig. 2), all soil C storage data were normalized (i.e., zero to one) and presented here as fractions of C storage at time of conversion from native grassland to annual cropland (shown as -250 years before time of soil sample collections).

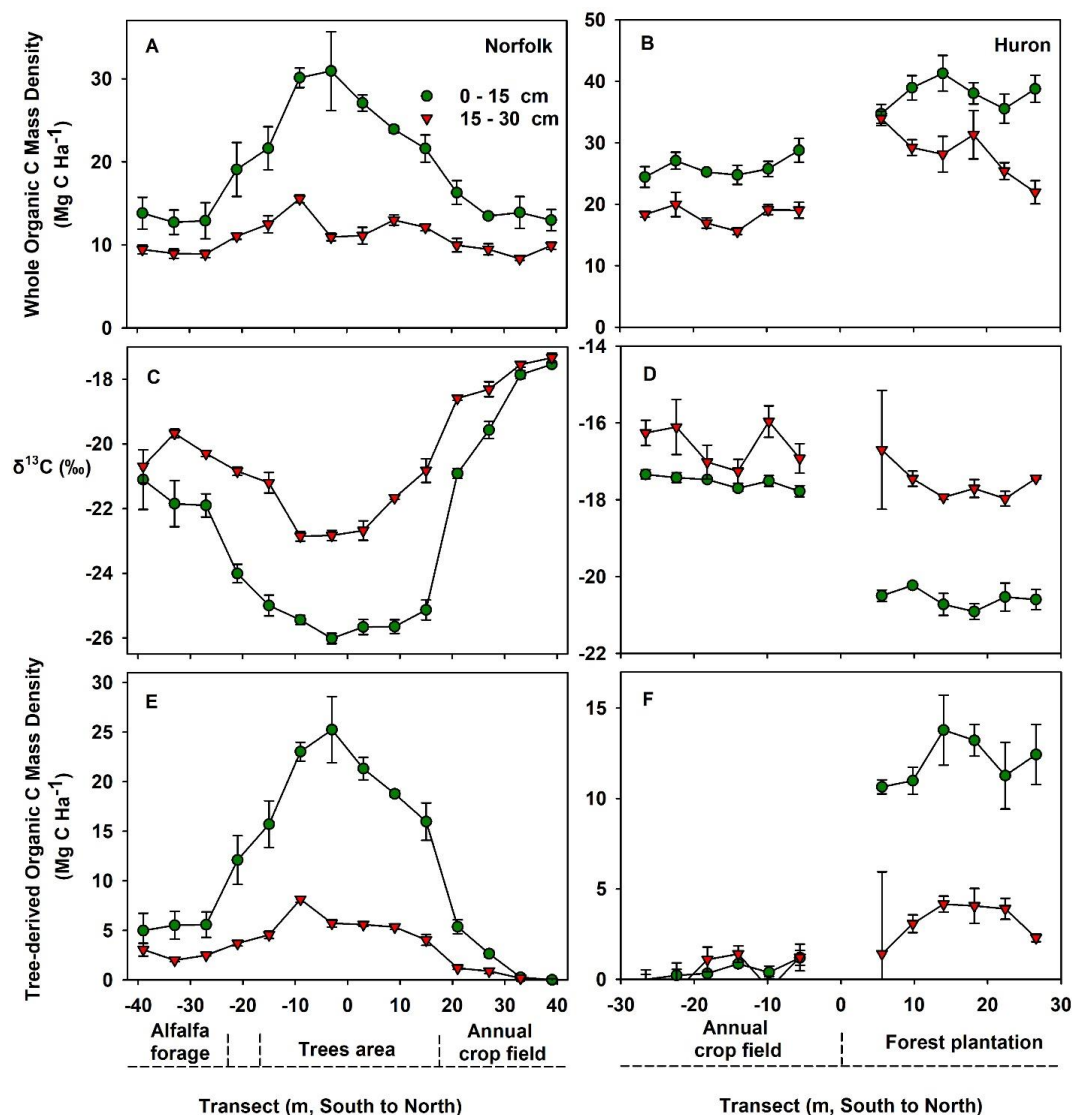


Fig. 4. (A, B) Soil organic carbon mass storage, (C, D) stable isotope ratios of organic C ($\delta^{13}C$), and (E, F) organic C mass derived from C3 plants across transects at Norfolk shelterbelt (left panels) and Huron forest plantation (right panels) for the 0 to 15 and 15 to 30 cm soil depth increments. Adjacent cropped fields were also included. Within the afforested areas in panels E and F, the reported organic C masses are primarily attributed to direct tree contributions. Contributions of tree-C to soil C storage were clearly discernable within the 0 to 15 cm depth increment. Note the difference vertical scales across panels. Error bars are standard errors of the means, with sample sizes of 4 for Huron and 3 for Norfolk.

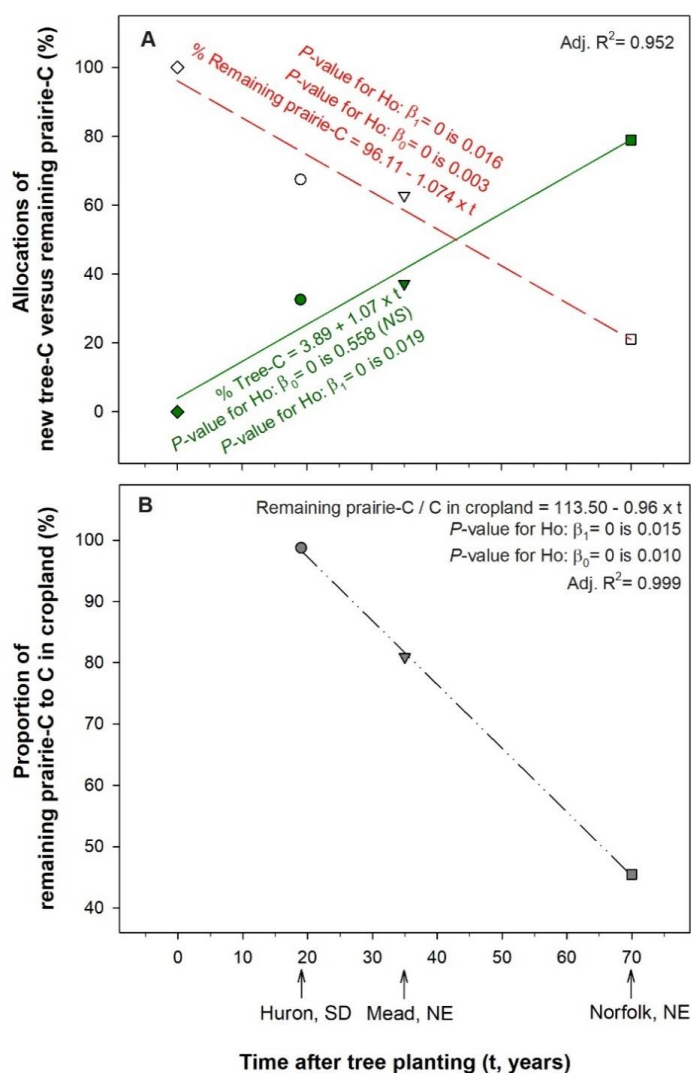


Fig. 5. Proportions of soil organic carbon within 0 to 15 cm depth increment (A) from tree-C versus remaining prairie-C relative to whole soil C stored directly beneath trees, and (B) remaining prairie-C in afforested soils relative to whole soil C in the adjacent croplands. It was inferred that all soil C different from new tree-C was preexisting soil C attributable to remaining prairie-C. (A) Mead data was recalculated from Hernandez-Ramirez et al. (2011) as compiled in Table 2. The tree-C source increased to become 79% of the whole soil C over 70 years after tree planting. (B) The proportion of prairie-derived C beneath trees declined over time to become less than half (45%) of the whole soil C in the adjacent annual croplands, which were assumed to be at steady state.

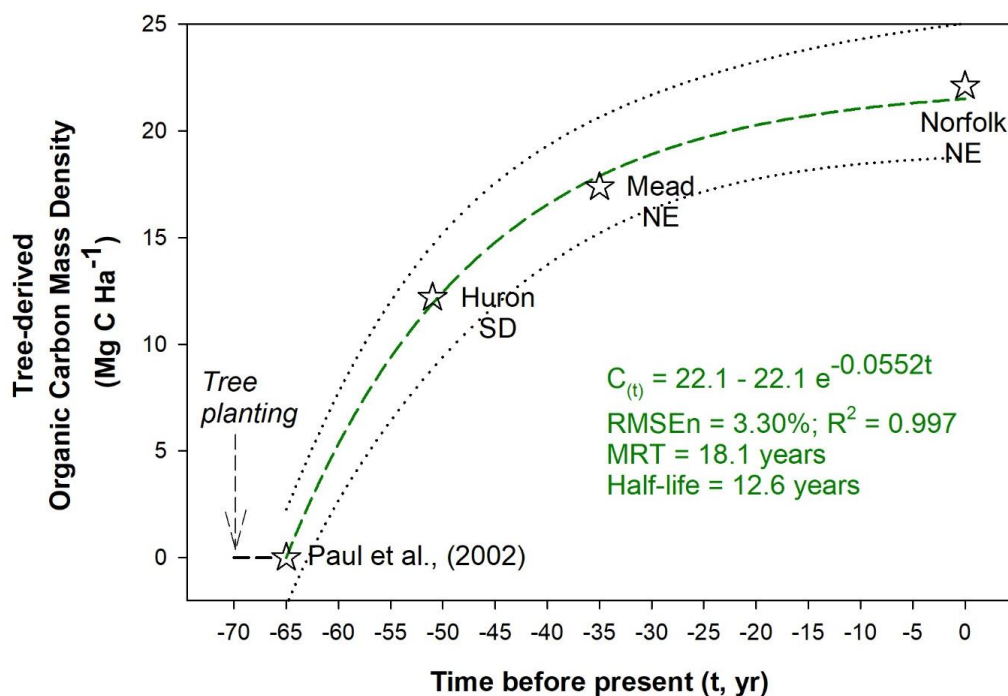


Fig. 6. Reconstruction of soil organic carbon storage within the 0 to 15 cm depth increment following land use conversion from annual cropland to afforestation United States. The arrow indicates the time of tree planting (-70 years). Based on a literature review by Paul et al. (2002), we included a lag phase of 5 years following tree planting. Huron and Norfolk data were derived from results presented in Fig. 4. Mead data was recalculated from Hernandez-Ramirez et al. (2011) as compiled in Table 2. This assemblage supports that afforested soils were approaching steady state at nearly 70 years after tree planting, as required for first-order kinetic modelling. The first-order kinetic model is depicted by the solid curvilinear fitting and equation in the general form $C_{(t)} = C_e + (C_o - C_e) e^{-kt}$, where k is the first-order kinetic rate constant equivalent to accretion rate under afforestation, and MRT stands for mean residence time. Normalized root mean square error (RMSEn) and coefficient of determination (R^2) for the k model are also provided. The 95% prediction bands of this k model are provided as dotted lines. This nonlinear trajectory describes and highlights the contribution of trees to soil C accrual.

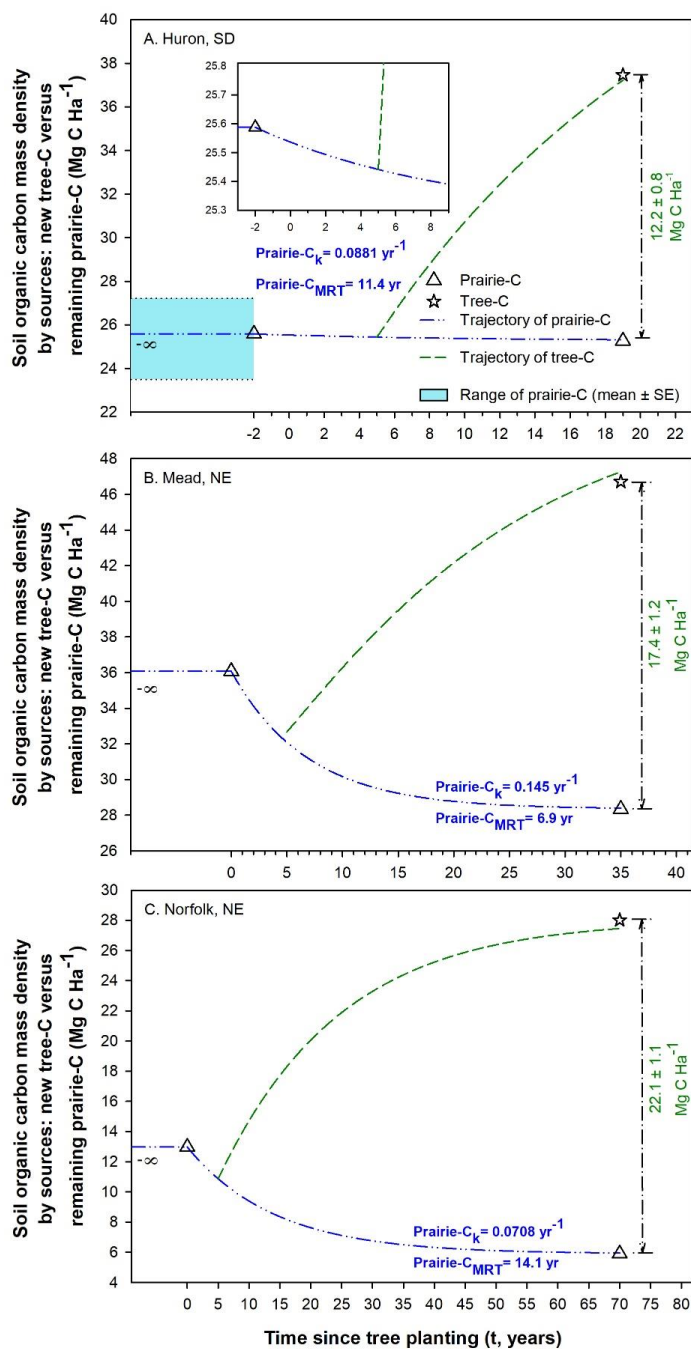


Fig. 7. Dynamics of net carbon accretion in afforested soils caused by simultaneous C gains from substantial tree-C contributions and smaller C losses from mineralization of remaining prairie-C. It was inferred that all soil C different from new tree-C was preexisting soil C attributable to remaining prairie-C. Time of tree planting was set at the year zero. Based on a literature review by Paul et al. (2002), we included a lag phase of 5 years following tree planting. The accretion trajectories of tree-C presented within each Panel were projected using the unified first-order model developed in Fig. 6. The magnitude of tree-C gains as well as the turnover rates (k) and mean residence times (MRT) of prairie-C trajectories are provided within each panel. The Huron site (Panel A) had an adjacent native grassland available, which here is provided as a reference and plotted prior to the time of conversion into annual cropland. Note the different x and y scales across panels.